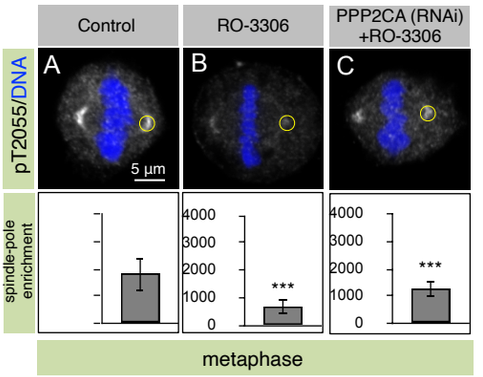

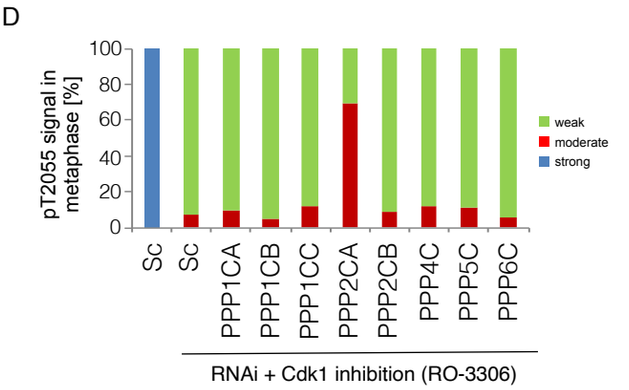

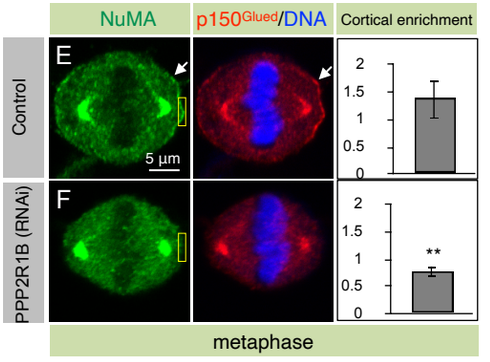

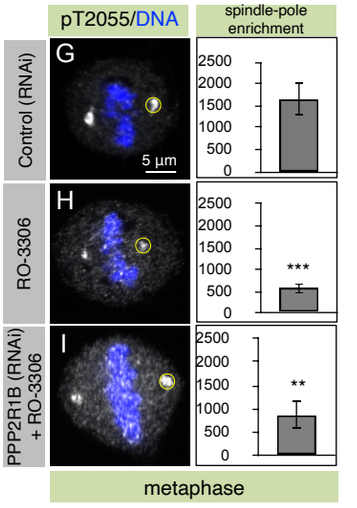

Supplementary Figure 1

PPP2CA and PPP2R1B are the catalytical and the scaffold subunit of PP2A involved in T2055 dephosphorylation

(A-C) HeLa cells in metaphase transfected with control siRNAs (A), treated with RO-3305 for 5 min (B), or transfected with PPP2CA siRNAs and were treated with RO-3306 for 5 min (C). Quantification of spindle pole signal is shown for 10 metaphase cells in each condition as in Figure 1. $p<0.0001$ between control and RO-3306 treated cells, and $p<0.0001$ between RO-3306 and PPP2CA siRNAs+RO-3306 cells; in this and other figures $p<0.0001$ is represented by *** and $p<0.01$ is represented by ** as calculated by two-tailed Student's t-test; error bars: s.d.).

(D) Metaphase HeLa cells transfected with control siRNAs, treated with Cdk1 inhibitor RO-3306 (10 μM) for 5 min, or transfected with siRNAs against eight catalytical PP2A subunits (as indicated) and acutely treated with RO-3306 for 5 min. Cells were fixed 72 hr of siRNAs transfection and stained with an antibody against pT2055. Stacked columns show the extent of pT2055 signal visually quantified using an epifluorescence microscope at the spindle poles, which were catagorized either weak as upon RO-3306 treatment (for example, see panel 'B'), strong as in control cells (for example, see panel 'A'), or moderate as in between weak and strong (for example, see panel 'C'). More than 200 cells were analyzed in each condition (see also Figure 1). Also, the depletion

efficiency for each siRNAs against all the catalytical subunit was estimated by western blot analysis (data not shown).

(E, F) HeLa cells in metaphase, as indicated, transfected with control siRNAs (E) or RNAi-against PPP2R1B scaffold subunit (F). Cells were fixed after 72 hr of siRNAs transfection and thereafter stained for NuMA and $p150^{Glued}$ (red). Quantification on the right shows the extent of cortical NuMA, which was significantly reduced in cells depleted of PPP2R1B by RNAi. ($p<0.0001$ between control and PPP2R1B siRNAs treated metaphase cells; $n>20$; error bars: s.d.).

(G-I) Metaphase HeLa cells transfected with control siRNAs (G), treated with Cdk1 inhibitor RO-3306 (10 μM) for 5 min (H), or transfected with PPP2R1B and treated with RO-3306 for 5 min (I). Cells were fixed after 72 hr of transfection and stained with an antibody against pT2055 (grey). Quantification on the right show extent of the pT2055 signal at the spindle poles. Note significantly reduced cortical pT2055 signal in cells treated by RO-3306. Also, note the stabilization of pT2055 signal in cells that are depleted of PPP2R1B and also briefly treated with RO-3306. ($p<0.0001$ between control and Cdk1 inhibitor RO-3306 treated cells and $p=0.0002$ between RO-3306 and PPP2R1B siRNAs+RO-3306 cells; $n=10$; error bars: s.d.).

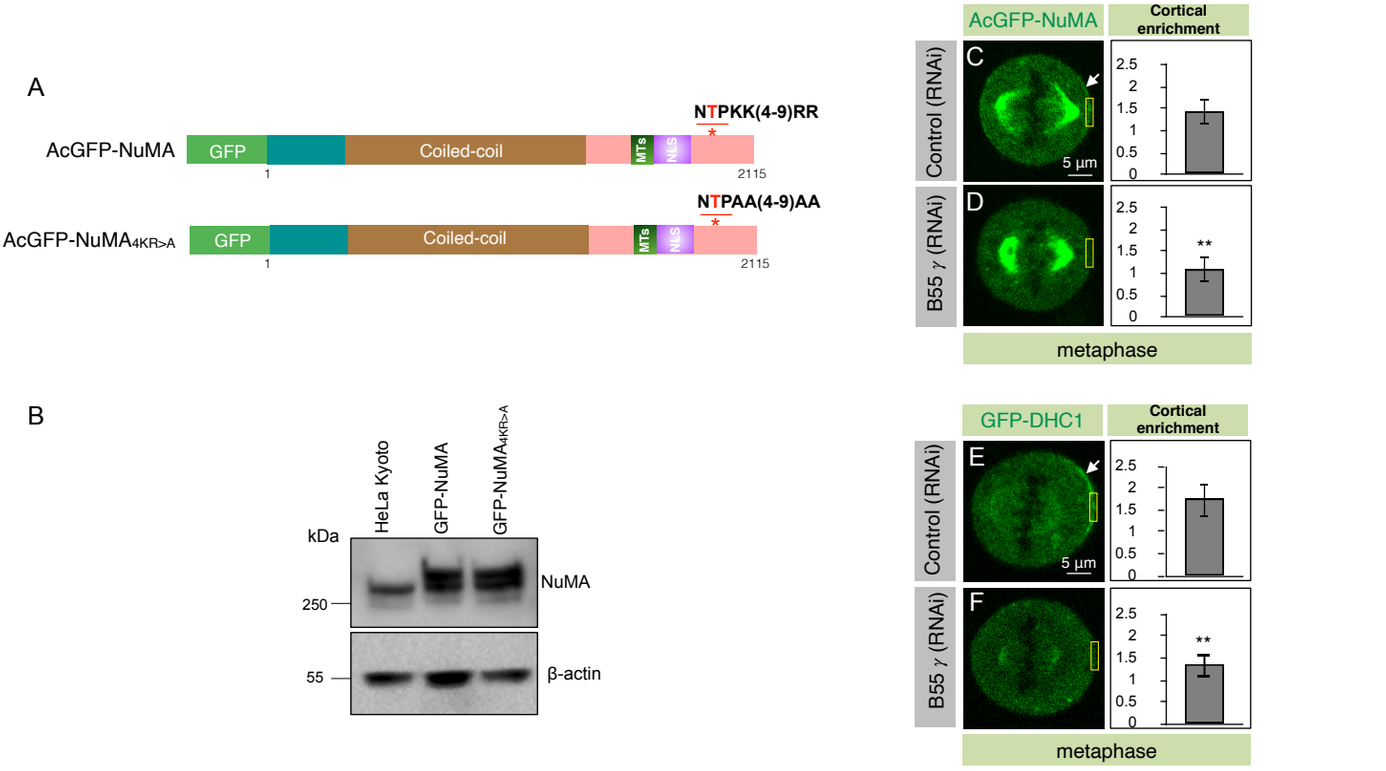

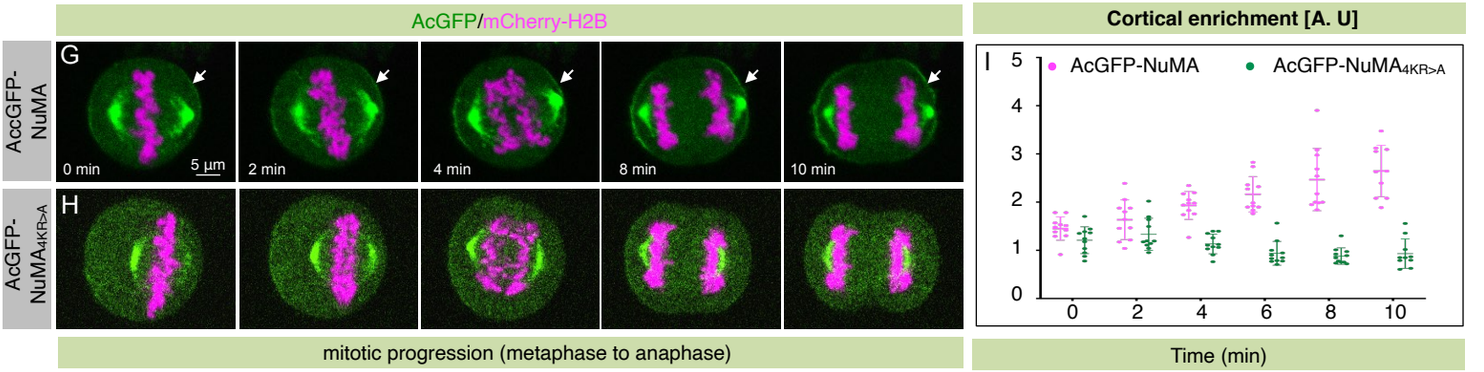

Supplementary Figure 2

Mutation in the polybasic residues in T2055 vicinity abolish cortical localization of NuMA

(A, B) Schematic of AcGFP-NuMA and AcGFP-NuMA$_{4KR>AA}$ construct with mono FLAG (FL) and AcGFP-tag at the N-terminus (A). Characterization of HeLa' Kyoto' line stably expressing AcGFP-NuMA and AcGFP-NuMA$_{4KR>A}$ by western blot analysis (B). In this and other panels, the molecular mass is indicated in kilodaltons (kDa) on the left.

(C-F) Images from the time-lapse confocal microscopy of HeLa' Kyoto' cells in metaphase that were stably expressing AcGFP-NuMA (C, D) or GFP-DHC1 (E, F) transfected with control siRNAs (C, E) or RNAi against B55γ (D, F). Quantification of cortical enrichment in metaphase is shown on the right for 10 cells in each condition; ($p=0.0042$ between Control and B55γ siRNA treated cells expressing AcGFP-NuMA, and $p=0.0075$ between Control and B55γ siRNA treated cells expressing GFP-DHC1; error bars: s.d.).

(G-I) Images from time-lapse microscopy of HeLa cells that were stably co-expressing AcGFP-NuMA and mCherry-H2B (G) or AcGFP-NuMA$_{4KR>A}$ and mCherry-H2B (H). The GFP signal is shown in green, and mCherry signal is in magenta. Note the significant loss of cortical NuMA in cells expressing AcGFP-NuMA$_{4KR>A}$. Quantification of cortical enrichment is shown on the right for cells undergoing mitotic progression from metaphase to anaphase; see Materials and Methods (I). $p=0.41$, 0.07, <0.0001, <0.0001, <0.0001 and <0.0001 between mCherry-H2B and AcGFP-NuMA and AcGFP-NuMA$_{4KR>A}$ for cortical GFP for 0, 2, 4, 6, 8 and 10 min as indicated; error bars: s.d.).

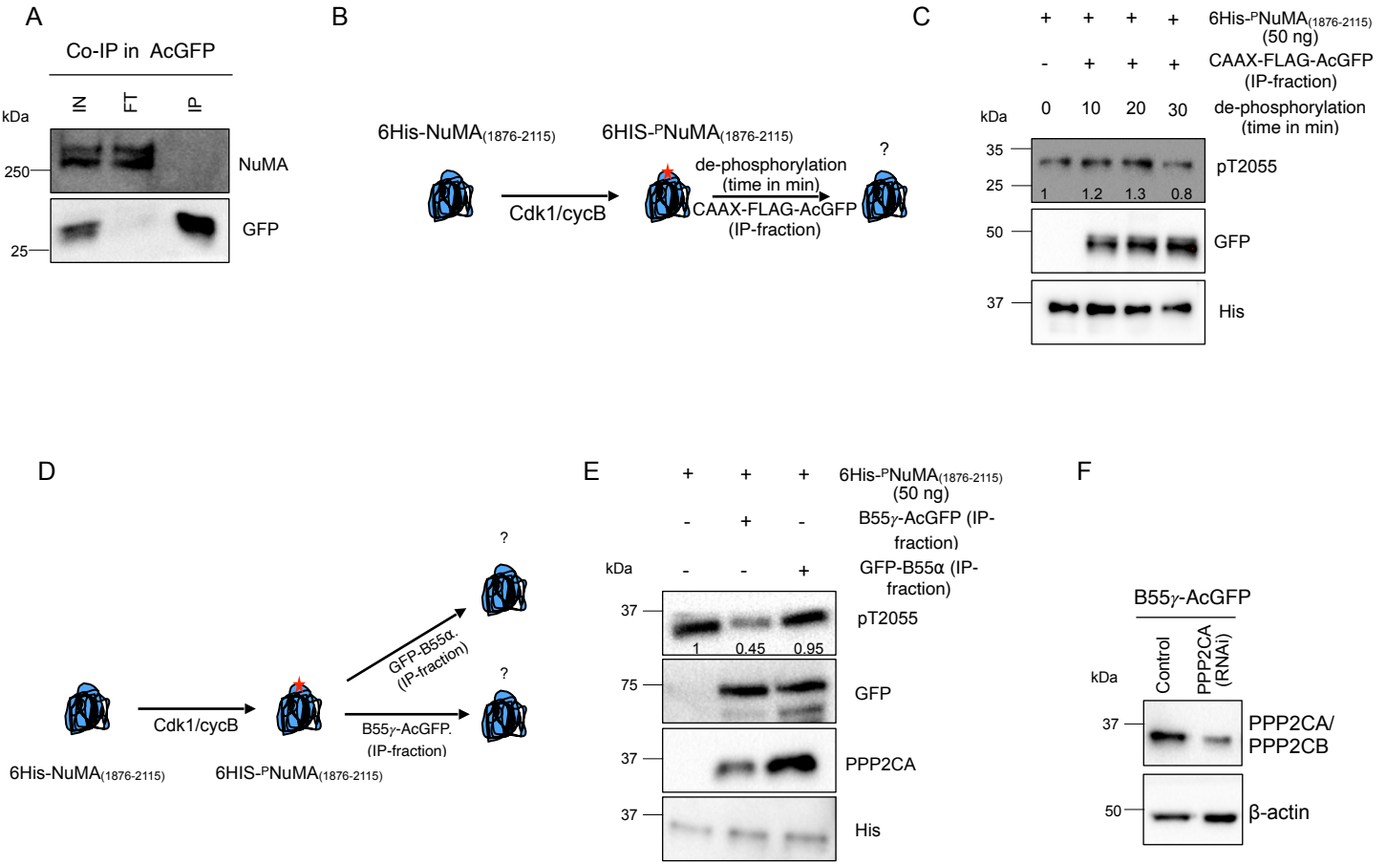

Supplementary Figure 3

PP2A-B55γ specifically dephosphorylates pT2055 in vitro

(A) Co-immunoprecipitation (IP) using GFP-Trap from Nocodazole arrested mitotic HeLa cells extracts expressing AcGFP. Resulting blots were probed for NuMA, and GFP as indicated. IN (1% of total), IP: 50% of the total. Please note that for GFP detection in the IP fraction, only 10% of the total IP fraction was loaded.

(B, C) Schematic representation of the *in vitro* dephosphorylation assay whereby Hexa-histidine-tagged $NuMA_{(1876-2115)}$ fragment [6HIS-$NuMA_{(1876-2115)}$] which was phosphorylated by Cdk1/cycB was incubated with the IP fraction from HeLa cells stably expressing CIBN-CAAX-FLAG-AcGFP [CAAX-FLAG-AcGFP] (B). Dephosphorylation reaction with Cdk1/cycB phosphorylated 6HIS-$NuMA_{(1876-2115)}$ with CAAX-FLAG-AcGFP IP fraction at a different times as indicated (C). Note that in this and other dephosphorylation experiments, values below the pT2055 western blot represent the band intensity with respect to the initial intensity value, which was kept as 1.

(D, E) Schematic representation of the *in vitro* dephosphorylation assay as mentioned above, however, dephosphorylation reactions were performed by either incubating with B55γ-AcGFP IP fraction or GFP-B55α IP fraction for 10 min (D). Dephosphorylation reaction with Cdk1/cycB phosphorylated 6HIS-$NuMA_{(1876-2115)}$ was performed either with the B55γ-AcGFP IP or with GFP-B55α IP (E). Please note almost negligible dephosphorylation potential of the B55α in contrast to B55γ.

(F) Western blot analysis of HeLa' Kyoto' line stably expressing B55γ-AcGFP and treated with control siRNAs (Control) or siRNAs against PPP2CA. Please note that PPP2CA antibody also recognizes PPP2CB, and thus the residual protein band may reflect PPP2CB as both proteins have similar molecular weight.

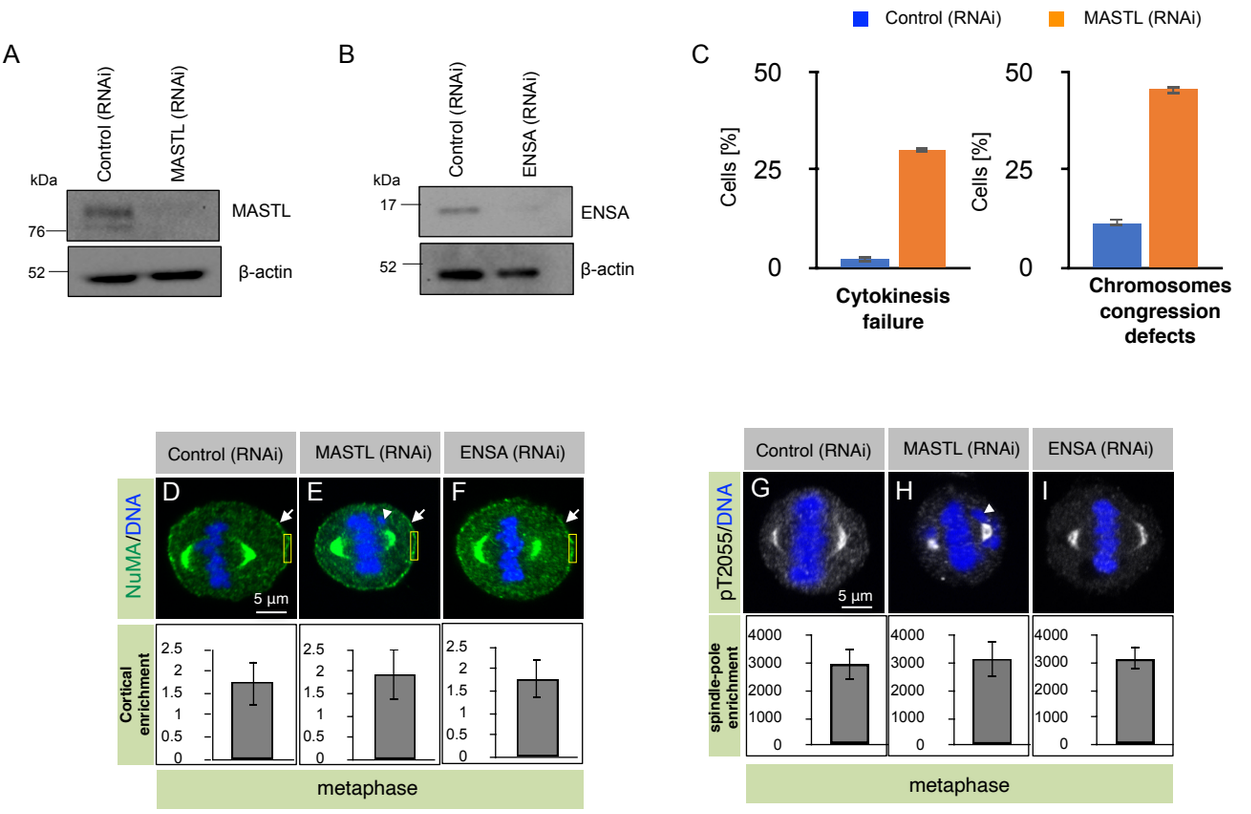

Supplementary Figure 4

Greatwall kinase MASTL or its regulatory subunit ENSA are not involved in pT2055 dephosphorylation

(A, B) Western blot analysis of MASTL (A) and ENSA (B) depletion by RNAi. β-actin was kept as a control.

(C) HeLa cells treated with control siRNAs or siRNAs against MASTL siRNAs. Cells were fixed after 60 hr of siRNAs transfection and thereafter scored for cytokinesis failure and chromosomes congression defects.

(D-F) HeLa cells treated with control siRNAs (D), MASTL siRNAs (E), or siRNAs against ENSA (F). Cells were fixed after 60 hr of siRNAs transfection and thereafter stained for NuMA (green). Note no significant change in the cortical NuMA levels in cells transfected with MASTL or ENSA siRNAs. Also, note chromosomes instability in cells that were treated with MASTL siRNAs, as shown by the arrowhead.

(G-I) HeLa cells treated with control siRNAs (G), MASTL siRNAs (H) or ENSA siRNAs (I). Cells were fixed after 60 hr of siRNAs transfection and thereafter stained for pT2055 (grey). Note no significant change in the spindle pole pT2055 levels in cells that were transfected with MASTL or ENSA siRNAs.

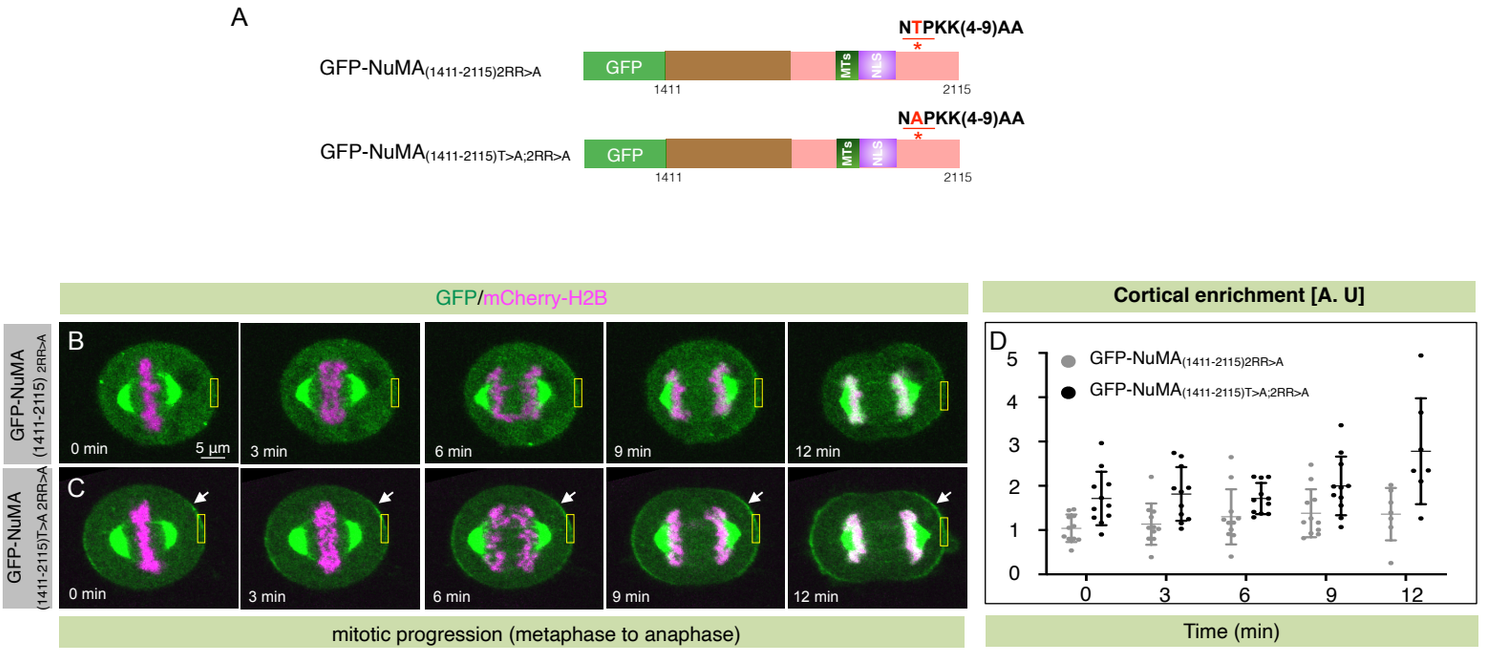

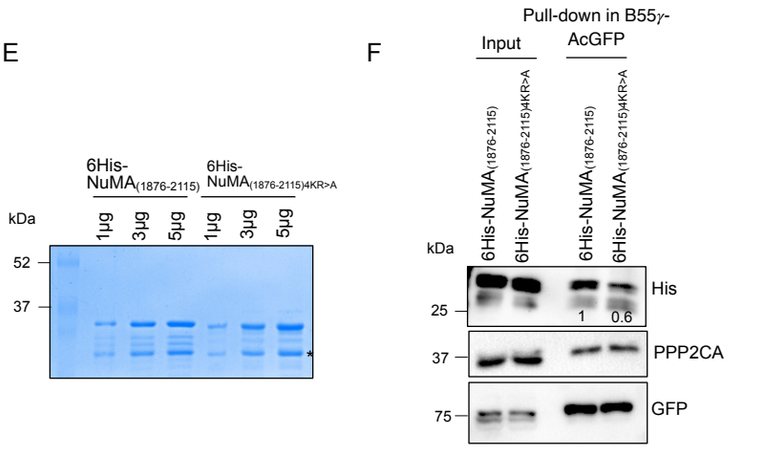

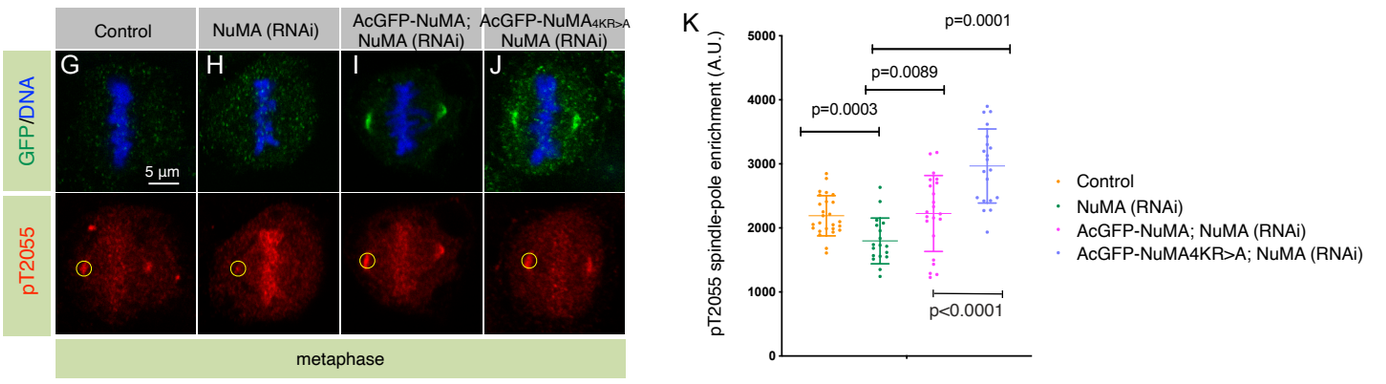

Supplementary Figure 5

Polybasic residues in the vicinity of T2055 are critical for NuMA localization at the cell cortex

(A) Schematic of AcGFP-NuMA$_{(1411\text{-}2115)2RR>A}$ and AcGFP-NuMA$_{(1411\text{-}2115)T>A;2RR>A}$ construct with mono FLAG (FL) and AcGFP-tag at the N-terminus.

(B, C) Images from time-lapse microscopy of HeLa cells stably expressing mCherry-H2B and were transfected either with GFP-NuMA$_{(1411\text{-}2115)2RR>A}$ (B) or GFP-NuMA$_{(1411\text{-}2115)T>A;2RR>A}$ (C). The GFP signal is shown in green, and the mCherry signal is in magenta. Note the significant loss of cortical NuMA in cells expressing GFP-NuMA$_{(1411\text{-}2115)2RR>A}$. Also, note the considerable rescue of the cortical signal in cells that were expressing GFP-NuMA$_{(1411\text{-}2115)T>A;2RR>A}$ construct wherein addition to the 2RR>A mutations, T2055 was mutated to alanine.

(D) Quantification of cortical enrichment on the right for cells that underwent metaphase to anaphase transition (shown in B, C); see Experimental procedures. $p<0.01$ between GFP-NuMA$_{(1411\text{-}2115)2RR>A}$ and GFP-NuMA$_{(1411\text{-}2115)T>A;2RR>A}$ at different time interval as indicated. (error bars: s.d.).

(E) Coomassie-stained gel for the wild-type [6HIS-NuMA$_{(1876\text{-}2115)}$] and mutated NuMA fragments [6HIS-NuMA$_{(1876\text{-}2115)4KR>A}$] that were generated and purified from *E.coli*. Please note that 6HIS-NuMA$_{(1876\text{-}2115)}$, and 6HIS-NuMA$_{(1876\text{-}2115)4KR>A}$ are unstable, therefore the occurrence of two species in Coomassie-stained gel.

(F) The above mentioned recombinant proteins were incubated with the mitotically synchronized HeLa cells extracts made from cells that were stably expressing B55γ-AcGFP followed by co-immunoprecipitation (IP) using GFP-Trap. Resulting blots were

probed for antibodies raised against 6HIS-tag, PPP2CA, and GFP as indicated. IN (1% of total), IP: 30% of the total. Please note significantly weak interaction between B55γ and 6HIS-NuMA$_{(1876\text{-}2115)4KR>A}$.

(G-K) HeLa' Kyoyo' cells in metaphase (G), cells treated with NuMA siRNAs targetting endogenous NuMA (H), cells stably expressing AcGFP-NuMA and treated with NuMA siRNAs targetting endogenous NuMA (I) and cells stably expressing AcGFP-NuMA4KR>A are treated with NuMA siRNAs targetting endogenous NuMA (J). Cells were fixed after 72 hr of siRNAs transfection and thereafter stained for pT2055 (red) and GFP (green). Quantification on the right reveals the spindle pole intensity of pT2055 under these conditions (K). Note AcGFP-NuMA or AcGFP-NuMA$_{4KR>A}$ are sufficiently phosphorylated by Cdk1 at T2055 in the absence of endogenous NuMA; error bars: s.d.

Table S1 siRNAs information

Gene	Purchased from	sequence(5'-3')
PPP1CA	Dharmacon Smartpool On target plus	GCAAGAGACGCUACAACAU, GAGCAGAUUCGGCGGAUCA, CAUCUAGGUUUCUACGAU, GAACGACCGUGGCGUCUCU
PPP1CB	Dharmacon Smartpool On target plus	GCAAAGUUAUGGUCGAUUU, GCUGAGCGAUUUCUAAUAA, GUGCUUAACUGUCUAAUAU, GAGAAGAGACUUAAUCCAA
PPP1CC	Dharmacon Smartpool On target plus	GCGGAGAGUUUGACAAUGC, CGAAUUAUGCGACCAACUG, UAGAUAAACUCAACAUCGA, UGACAUCCAUGGACAAUAC
PPP2CA	Dharmacon Smartpool On target plus	CCGGAAUGUAGUAACGAUU, ACAUUAACACCUCGUGAAU, UCAUGGAACUUGACGAUAC, CAGGUAGAGCUUAAACUAA
PPP2CB	Dharmacon Smartpool On target plus	CACGAAAGCCGAAAAUUA, UUUAGUAGAUGGACAGAUA, CCAGAACGCAUUACAAUAU, GAACCAGGCUGCUAUCAUG
PPP4C	Dharmacon Smartpool On target plus	GCACUGAGAUCUUUGACUA, GACAAUCGACGAAAGCAA, GCACUUAAGGUUCGCUAUC, GGAGCCGGCUACCUAUUUG
PPP5C	Dharmacon Smartpool On target plus	GGGCGUGAGCUGUCAGUUU, GACCAACCCCUAUAUAUAUUU, UGUACGAGCUCUUUAGCGA, GAUCUACGGUUUCGAGGGU
PPP6C	Dharmacon Smartpool On target plus	CUAAAUGGCCUGAUCGUAU, CGCUAGACCUGGACAAGUA, GUUUGGAGAACCUUCACUUA, CGAACGGAAUCAGGAAAUU
PPP2R1A	Dharmacon Smartpool On target plus	AGGCGGAACUUCGACAGUA, AAACUUAACUCCUUGUGCA, GUUCACAGAGCUCCAGAAA, GAGCUUCUGCCUUUCCUUA
PPP2R1B	Dharmacon Smartpool On target plus	GACCAAUUCUAGAUACCAA, GACCAAUUCUAGAUACCAA, GCUCUAGCUUCUGUAAUUA, GACCGAAGUGAAUUGUUG
PPP2R2A	Dharmacon Smartpool On target plus	CAUACCAGGUGCAUGAAUA, GUAUAGAGAUCCUACUACA, GCAAGUGGCAAGCGGAAAGA, AGACAUAACCCUAGAAGCA
PPP2R2B	Dharmacon Smartpool On target plus	UCGAUUACCUGAAGAGUUU, GGGUCGGGUUGUAAUAUUU, GAAUGCAGCUUACUUUCUU, CCACACGGGAGAAUUACUA
PPP2R2C	Dharmacon Smartpool On target plus	CGGAGGAUCUUUGCCAAUG, GAUACAACCUGAAGGAUGA, CCAACAACCUGUACAUCUU, GAAGAUUACCGAACGAGAU
PPP2R2D	Dharmacon Smartpool On target plus	GUAGGUCCUUCUUCUCAGA, UCGGAUAGCGCCAUCAUGA, GAGACUACCUGUCGGUGAA, GAGAACGACUGCAUCUUUG
PPP2R3A	Dharmacon Smartpool On target plus	GGAAGGCUUUGAAGAUUAU, CAGAAUGGCUCACAUCUUC, CCAUAAACAUUCCACGGUU, GGAGAAAGUUGCUGAAUAA
PPP2R3B	Dharmacon Smartpool On target plus	CGGCCGAGGAGUACGACAU, GGUCAAGCCGAGGACUGAA, GGAAGAUCACGCUGCAGGA, GGACAGCAUGGCCAUCGAG
PPP2R3C	Dharmacon Smartpool On target plus	AGAAGAACUCUCACGCUAU, GCGAUGAUCAAUUACGAAA, CCACCAUUCUAAUCGAUUU, AAGAAUAGGACUCAGUUUA
PPP2R4	Dharmacon Smartpool On target plus	GCAGUUCGCAGCUGAUAGA, UGGAGUGUAUCCUGUUUAU, GAUGAAGACUGGCCCAUUU, CCAACCAGCUGUGGAACAU
PPP2R5A	Dharmacon Smartpool On target plus	GCUCAAAGAUGCCACUUCA, CAAUACAAGUGCCGAAUAA, UGAAUGAACUGGUUGAGUA, GGAAAUGAAUGGCAAGCUU
PPP2R5B	Dharmacon Smartpool On target plus	CGCAUGAUCUCAGUGAAUA, UCAAGUCGCUGUCUGUCUU, CAAACCAUCGUAUCACUGA, GAACAAUGAGUAUAUCCUA
PPP2R5C	Dharmacon Smartpool On target plus	GGAUUUGCCUUACCACUAA, GGAAGAUGAACCAACGUUA, CAUCAGAAUUUGUGAAGAU, CAGAAGUAGUCCAUAUGUU
PPP2R5D	Dharmacon Smartpool On target plus	GUACAUCGACCAGAAGUUU, UCCAUGGACUGAUCUAUAA, UGACUGAGCCGGUAAUUGU, GUAGGCAGAUCAACCACAU
PPP2R5E	Dharmacon Smartpool On target plus	UUAAUGAACUGGUGGACUA, GCACAGCUGGCAUAUUGUA, GACACGCUAUCUGAUCUUA, GGAUAAAGUAGACGGUUU
ENSA	Life technology	GAGGCAAAGCUAAAGGCCAtt
ENSA	Life technology	GCCUAGGACAAAAGCCUGGtt
MASTL	Invitrogen	ACGCCTTATTCTAGCAAATTA
MASTL	Invitrogen	CAGGACAAGTGTTATCGCTTA
PPP2R1A	Life technology	CUUCGACAGUACUUCCGGAtt
PPP2R1B	Life technology	GACCAAUUCUAGAUACCAAtt
PPP2R2A	Life technology	GAGCUAACAGAGGUGAUUAtt
PPP2R2B	Life technology	GGGACUACUUGACCGUCAAtt
PPP2R2C	Life technology	GAUACAACCUGAAGGAUGAtt
PPP2R2D	Life technology	UCAUGACCGGGUCCUAUAAtt
PPP2R3A	Life technology	CGAUCUGUCUCGAUACAAUtt
PPP2R3B	Life technology	CCUCGACCACGAGCAGAAAtt
PPP2R3C	Life technology	CGAUGAUCAAUUACGAAAAtt
PPP2R4	Life technology	GGAUUCAUCCUUACCCUCAtt
PPP2R5A	Life technology	GCCUAGCAUUGCAAAACGAtt
PPP2R5B	Life technology	GAACAAUGAGUAUAUCCUAtt
PPP2R5C	Life technology	GGCUUGAGAGCUUACAUCAtt
PPP2R5D	Life technology	GCCGUGAUGUUGUCACUGAtt
PPP2R5E	Life technology	CACGCUAUCUGAUCUUAAAtt
NuMA 3'UTR	Eurogentec	CAGTACCAGTGAGTGGCCCCACCTG
NuMA 3'UTR	Invitrogen	CCUCUGGAUCUAGAAGGGACCAUAA